Chemosphere 286 (2022) 131817

Contents lists available at ScienceDirect

Chemosphere

journal homepage: www.elsevier.com/locate/chemosphere

Vanadium removal from mining ditch water using commercial iron products and ferric groundwater treatment residual-based materials☆

Ruichi Zhang [a], Jinmei Lu [b], Mark Dopson [c], Tiina Leiviskä [a,*]

[a] Chemical Process Engineering, P.O. Box 4300, FIN-90014, University of Oulu, Oulu, Finland
[b] Department of Technology and Safety, UiT—The Arctic University of Norway, N-9037, Tromsø, Norway
[c] Centre for Ecology and Evolution in Microbial Model Systems, Linnaeus University, 39182, Kalmar, Sweden

HIGHLIGHTS

- A mining ditch water contained high concentration of vanadium (4.66–6.85 mg/L).
- Commercial and waste iron products efficiently removed vanadium from water.
- No hazardous elements leached into the treated water.
- Akaganéite-based sorbent proved to have the best performance in column mode.

GRAPHICAL ABSTRACT

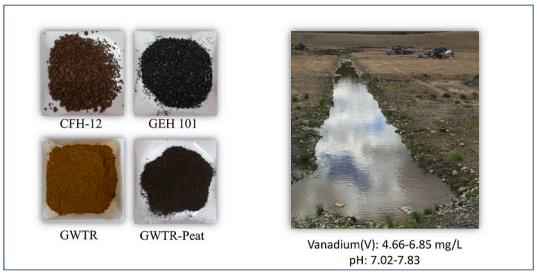

ARTICLE INFO

Handling Editor: Derek Muir

Keywords:
Vanadium uptake
Mining effluent
Iron sorbent
Waste iron product
Hazard quotient

ABSTRACT

Removal of vanadium from liquid waste streams protects the environment from toxic vanadium species and promotes the recovery of the valuable metal. In this study, real mining ditch water was sampled from a closed vanadium mine (V–Fe–Ti oxide deposit, Finland) and used in sorption experiments at prevailing vanadium concentration (4.66–6.85 mg/L) and pH conditions (7.02–7.83). The high concentration of vanadium in the water represents a potential health concern according to the initial risk assessment carried out in this study. Vanadium was efficiently removed using four different iron sorbents: ferric oxyhydroxide with some goethite (CFH-12), poorly crystallized akaganéite (GEH 101), ferric groundwater treatment residual (GWTR), and GWTR-modified peat (GWTR-Peat). Higher dosage (6 g/L with 24 h contact time) and longer contact time (72 h using 1 g/L dosage) resulted in removal efficiencies of higher than 85%. Kinetic data were well represented by the Elovich model while intra-particle diffusion and Boyd models suggested that the sorption process in a real water matrix was significantly controlled by both film diffusion and intra-particle diffusion. Column studies with CFH-12, GEH 101, and GWTR-Peat showed that the breakthrough started earlier with the mining ditch water compared to a synthetic vanadium solution (investigated only with CFH-12), whereas GEH 101 proved to have the best performance in column mode. The Thomas and Yoon-Nelson column models were found to agree with the experimental data fairly well with the 50% breakthrough time being close to the experimental value for all the studied sorbents.

☆ Declarations of interest: none.

* Corresponding author.
E-mail addresses: ruichi.zhang@oulu.fi (R. Zhang), jinmei.lu@uit.no (J. Lu), mark.dopson@lnu.se (M. Dopson), tiina.leiviska@oulu.fi (T. Leiviskä).

https://doi.org/10.1016/j.chemosphere.2021.131817
Received 9 February 2021; Received in revised form 1 June 2021; Accepted 4 August 2021
Available online 6 August 2021

1. Introduction

Iron materials are excellent sorbents due to their strong chemical affinities for various water pollutants, their large specific surface area and possibility of reuse. Different iron materials such as goethite (Liu et al., 2013), magnetite (Hu et al., 2004), akagenéite (Yusan and Akyil, 2008) and amorphous iron hydroxide (Dixit and Hering, 2003) have been used for the removal of arsenic, uranium, chromium and phosphate from water. These iron products contain hydroxyl groups, which can form complexes with various ions (Liu et al., 2013; Zelmanov and Semiat, 2015). Numerous studies have also developed low-cost sorbents impregnated with iron particles for the removal of different contaminants from water (Aryal et al., 2010; Wang et al., 2016b).

Besides commercial iron materials, the utilization of waste iron from various industries has gained a lot of interest in recent years (Grace et al., 2016; Janoš et al., 2011; López-Delgado et al., 1998; Zhang et al., 2015). These waste iron materials from the steel industry, the blast furnace process and iron ore tailings have been used as sorbents in water purification (Giri et al., 2011; Lee et al., 2003; López-Delgado et al., 1998; Park et al., 2008). In addition, the water treatment residuals (WTRs) generated during the Al/Fe coagulation process in water treatment plants have been studied in terms of environmental remediation and water purification (Jacukowicz-Sobala et al., 2015). Fe-WTRs have been used directly as sorbents to successfully remove metal cations such as Cu(II), Pb(II), Cd(II), Zn(II) (Castaldi et al., 2015; Chiang et al., 2012) and anionic contaminants such as phosphate (Gao et al., 2013) and arsenic (Chiang et al., 2012). A few studies have also applied pretreatment methods on Fe-WTRs and Al-WTRs, for example heat treatment, sequential thermal and acid activation (Wang et al., 2011, 2016a). Iron has also been extracted from a ferric groundwater treatment residual (Fe-GWTR) using hydrochloric acid; the iron solution formed was used to replace synthetic iron chemical in the preparation of iron-modified peat (Zhang et al., 2019) and kaolin-supported zerovalent iron (Bello et al., 2019) for vanadium sorption.

Vanadium has a wide variety of applications, with the majority being used as a steel additive. Vanadium-containing wastewaters may be a potential source for the recovery of valuable vanadium; however, waste streams may cause environmental concerns due to the potential toxicity of vanadium. It can disperse and persist in the environment to a greater degree than other contaminants (Watt et al., 2018) and high concentrations can cause toxicity to aquatic organisms. For instance, population growth in the brackish water hydroid *Cordylophora caspia* was significantly impaired by 2 mg/L vanadium over a 10-day exposure period (Teng et al., 2006). Consequently, some countries have set the limit value for vanadium in water, e.g. Italy has set a limit of 140 μg/L (Crebelli and Leopardi, 2012) and California has a notification level of 50 μg/L (Wright and Belitz, 2010). Though many studies have explored the carcinogenic potential of vanadium, there is currently no conclusive evidence for the associated health risks (Yang et al., 2017).

Different methods have been studied for vanadium removal, such as ion exchange (Chen et al., 2020; Dą;browski et al., 2004; Keränen et al., 2015), membrane filtration (Lazaridis et al., 2003; Melita and Gumrah, 2010), sorption (Leiviskä, 2021) and bioremediation (He et al., 2021; Shi et al., 2020; Wang et al., 2021; Zhang et al., 2021). Nevertheless, the sorption of vanadium is considered one of the most cost-effective technologies. However, most of the studies have used synthetic vanadium solutions as the water matrix and studies using real wastewater are very limited. Although various sorbents have demonstrated excellent vanadium sorption capacity, it has been rarely studied how sorbents cope with the challenges of real wastewaters, i.e. in the presence of multiple ions. Besides, successful vanadium separation from a real wastewater matrix constitutes a prerequisite for the potential of vanadium recovery from waste streams, which would have both economic and environmental benefits.

In the present study, the health risk from exposure to vanadium-containing mining ditch water was firstly assessed using a non-carconogenic health risk assessment approach. Then four different iron-based materials, comprising two commercial granulated iron products (CFH-12 and GEH 101) and two ferric groundwater treatment residual-based products (GWTR and GWTR-Peat), were selected and compared for vanadium removal from mining ditch water. The sampled mining ditch water was directly used in the experiments at prevailing vanadium concentration (4.66–6.85 mg/L) and pH conditions (7.02–7.83). Both batch and column studies were conducted and the ability of different models to fit the experimental data was investigated. X-ray photoelectron spectroscopy (XPS) was used for the characterization of materials before and after sorption. This study provides valuable information about the suitability of iron-based materials to remove vanadium from real mining-influenced waters.

2. Materials and methods

2.1. Risk assessment from vanadium exposure in the mining ditch water

The non-carcinogenic risk is represented in terms of the hazard quotient (HQ), which is defined as the ratio of chronic daily intake (CDI) to the reference dose (Yang et al., 2017). The HQs from vanadium exposure through dermal contact and ingestion routes were calculated

Table 1
Properties of the sorbents.

	CFH-12	GEH 101	GWTR	GWTR-Peat
Supplier/source	Kemira Oyj	GEH Wasserchemie	Finnish groundwater treatment plant	Zhang et al. (2019)
Full name	Ferric oxyhydroxide	Ferric hydroxide containing β-FeOOH and $Fe(OH)_3$	Ferric groundwater treatment residual	Ferric groundwater treatment residual modified peat
Physical form	Granular	Granular	Fine powder	Powder
Particle size	0.9 mm (D_{50})[a]	0.2–2.0 mm[a]	N/A	N/A
Fe content	44%[a]	61%[a]	57.6%[c]	14.6%
Surface area	241.8 m^2/g (washed)[b]	298.1 m^2/g (washed)[b]	295.6 m^2/g	53.4[d]
BJH pore volume	0.1001 cm^3/g (washed)[b]	0.2868 cm^3/g (washed)[b]	0.08 cm^3/g	0.392 cm^3/g[d]
Pore width	3.3 nm[b]	3.3 nm[b]	5.0 nm	29.4 nm[d]
Vanadium sorption capacity (mg/g)	34[b]	22[b]	27	12

[a] Obtained from the manufacturer.
[b] Obtained from Leiviskä et al. (2019).
[c] Obtained from Bello et al. (2019).
[d] Obtained from Zhang et al. (2019); sorption capacity of GWTR and GWTR-Peat was obtained by studying the effect of initial vanadium concentration on the vanadium removal (details provided in the Supplementary material).

for the mining ditch water before the sorption experiment using the methods in Çelebi et al. (2014). Detailed description of the methodology is provided in the Supplementary material. The calculated HQ was compared to 1 with HQ values > 1 presenting a risk for people exposed to it and there is no risk if then the HQ is ≤ 1.

2.2. Raw materials, chemicals and mining ditch water analysis

Four different sorbents (Table 1) were selected to treat the mining ditch water in batch tests. CFH-12 is granulated ferric oxyhydroxide that also contains some goethite and gypsum. GEH 101 is ferric hydroxide containing akaganéite (β-FeOOH) and ferrihydrite. CFH-12 and GEH 101 were washed several times with Milli-Q ultrapure water and dried at 60 °C for 24 h before use. Ferric groundwater treatment residual (GWTR) was collected from a Finnish groundwater treatment plant, dried at 40 °C for 72 h, and then ground with a hand mortar. The major components of GWTR were FeO (74.06 wt %), SiO_2 (12.46 wt %), MnO (5.06 wt %), P_2O_5 (2.37 wt %), CaO (1.18 wt %), Ba (1910 ppm) and Gd (973 ppm) (Bello et al., 2019). GWTR-Peat was prepared according to our previous study (Zhang et al., 2019) and contained the following major inorganic components: Fe_2O_3 (41.54 wt %), SiO_2 (3.00 wt %), SO_3 (1.71 wt %) and P_2O_5 (1.29 wt %). The synthetic vanadium solution was prepared by dissolving $NaVO_3$ (Sigma-Aldrich) in Milli-Q ultrapure water without pH adjusement.

Vanadium-containing mining ditch water was sampled from the closed Mustavaara mining site (Finland). The water was sampled from the stream which was in contact with the atmosphere. The pH and conductivity of the water were measured using a pHenomenal® pH 1000 L (VWR) pH meter and a Mettler Toledo conductivity meter, respectively. The sampled water was then stored in a cold room and taken to room temperature (approx. 21 °C) 24 h before the use. The mining ditch water was used in the sorption experiments at prevailing vanadium concentration and pH conditions. The collected water and selected water samples after batch sorption were sent for comprehensive elemental analysis (Eurofins Scientific). Metals were measured using inductively coupled plasma mass spectrometry (ICP-MS) (Thermo Scientific) according to the standard method (SFS-EN ISO 17294–2:2016). Sulfate, chloride and fluoride were measured using ion chromatography (SFS-EN ISO 10304–1:2009). Ammonium, phosphate, nitrate and nitrite were measured with a continuous flow analyser (SFS-EN ISO 13395:1997, SFS-EN ISO 11732:2005, SFS-EN ISO 15681–2:2005). The MINEQL program (version 5.0) was used to calculate chemical speciation in the mining ditch water.

2.3. Effect of sorbent dosage

The effect of dosage (1–6 g/L) was investigated (pH 7.02, initial vanadium concentration 4.66 mg/L) at a room temperature of 21 °C. A certain amount of sorbent was weighed into 50 mL Falcon tubes and 30 mL of mining ditch water was added. The tubes were shaken for 24 h in a horizontal rotary shaker. After sorption, the mixture was centrifuged for 10 min (Jouan C4.12, 2500 rpm, ~800×*g*). The supernatant was separated and sent for vanadium analysis using inductively coupled plasma optical emission spectrometry (ICP-OES). All the experiments were performed in duplicate.

2.4. Effect of contact time and kinetic modelling

Vanadium removal from mining ditch water was carried out for various contact times (1–72 h) with a constant sorbent dosage (1 g/L) at room temperature (21 °C). Otherwise, the batch experiment procedure was as described in section 2.3. For comparison, modelling of adsorption kinetics was also performed for the adsorption of vanadium from synthetic vanadium solutions (50 mg/L, pH 6.85). The experiments were conducted with contact times of 10 min–72 h at a constant sorbent dosage (5 g/L) for GWTR and GWTR-Peat. For CFH-12 and GEH 101, the experimental data was mostly acquired from a previous study (Leiviskä et al., 2019), except the experiments with 10–30 min contact time were conducted in this study. All tests were performed in duplicate at room temperature (21 °C). The batch experiment procedure was as described in section 2.3.

The data were then fitted with the pseudo-first-order (PFO, Eq. (1)) (Lagergren, 1898), pseudo-second-order (PSO, Eq. (2)) (Blanchard et al., 1984) and Elovich models (Eq. (3)) (Roginsky and Zeldovich, 1934):

$$q_t = q_e\left(1 - e^{-k_1 t}\right) \tag{1}$$

$$q_t = \frac{q_e^2 k_2 t}{1 + k_2 q_e t} \tag{2}$$

$$q_t = \frac{1}{\beta}\ln(1 + \alpha\beta t) \tag{3}$$

where q_e is the equilibrium vanadium sorption amount (mg/g); q_t is the vanadium sorption amount (mg/g) at any time t (min); k_1 is the PFO rate constant (1/min); k_2 is the PSO rate constant (g/mg × min) that can be calculated from the slope of the fitting curves; α is the initial rate constant (mg/(g × min)); and β is the desorption constant (g/mg) related to the Elovich model. To investigate the sorption process further, the experimental data were also fitted with the intra-particle diffusion model (Eq. (4)) (Weber and Morris, 1963) and Boyd model (Eq. (5) and Eq. (6), only for data of synthetic vanadium solutions) (Boyd et al., 1947; Edebali, 2019).

$$q_t = k_i t^{0.5} + C \tag{4}$$

$$B_t = 2\pi - \frac{\pi^2 F}{3} - 2\pi\left(1 - \frac{\pi F}{3}\right)^{0.5} \quad when\ 0 \le F \le 0.85 \tag{5}$$

$$B_t = -0.4977 - \ln(1 - F) \quad when\ 0.86 \le F \le 1 \tag{6}$$

where q_t is the sorption capacity (mg/g) at any time t (min); k_i is the intra-particle rate constant (mg/g × $min^{½}$); and C is a constant related to the thickness of boundary layer. F is the ratio of q_t/q_e of Boyd model, where q_e is the equilibrium sorption amount (mg/g). The Boyd model is obtained by plotting B_t versus time t.

2.5. Characterization

The surface area and pore size distribution of GWTR were measured by the Brunauer-Emmett-Teller (BET) and Barrett-Joyner-Halenda (BJH) methods using the N_2 adsorption technique with an ASAP 2020 surface area and porosity analyser (Micromeritics). Before analysis, the sample was outgassed in a vacuum for 12 h at 100 °C. An X-ray fluorescence (XRF) spectrometer (Bruker AXS S4 Pioneer) was used to analyse the chemical composition of GWTR-Peat. Prior to analysis, the samples were ground using a mortar and pestle into very fine particles, except the GWTR-Peat sample was ground using a WC/Co mill and balls (MiniMill II). The pressed pellet was prepared for analysis using boric acid as binder under a hydraulic pressure of 10 metric tons. The X-ray diffraction (XRD) measurement of GWTR was performed with a RIGAKU Mini-flex 600 X-ray powder diffractometer equipped with Cu-kα radiation. The sample was measured in the 2θ range of 2–75° with a step size of 0.05. The morphology of the untreated and treated samples was characterized using field emission scanning electron spectroscopy (FESEM, Zeiss Sigma). The samples were coated with platinum (Jeol Vacuum Evaporator JEE-420).

XPS analysis was performed for fresh and used sorbents using a Thermo Fischer Scientific ESCALAB 250xi with a monochromatic Al Kα source (1486.6 eV). The used sorbents were recovered from the batch experiments (dosage 1 g/L; pH 7.58; contact time 72 h) and washed several times with Milli-Q ultrapure water before being dried at 60 °C. The charge correction was made by setting the binding energy of

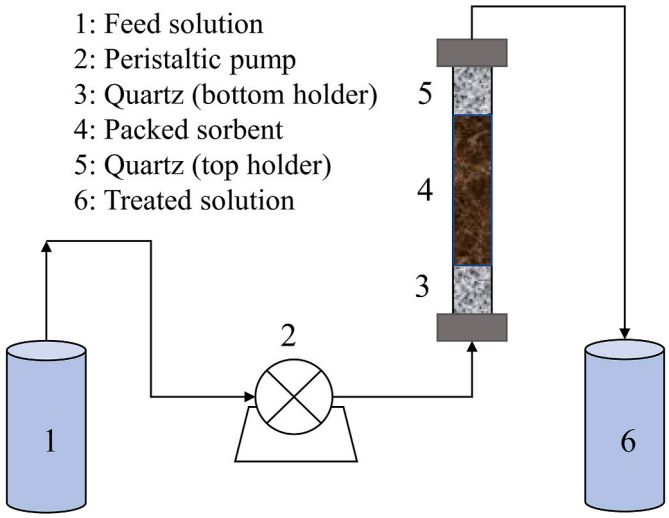

Fig. 1. Experimental setup of the fixed bed system.

adventitious carbon to 284.8 eV.

2.6. Column studies

Based on the sorption performance in the batch experiments, CFH-12, GEH 101 and GWTR-Peat were selected for the fixed-bed column studies (experimental setup shown in Fig. 1). All the experiments were carried out at room temperature (21 °C). A preliminary experiment using two columns of CFH-12 with synthetic vanadium solution (initial vanadium concentration 5.18–6.75 mg/L; pH 6.0) and different bed depths was conducted first to investigate its sorption behavior in column mode. The columns (inner diameter 19 mm; height 30 cm) were firstly packed with quartz in the bottom (particle size 0.5–1 mm; height ~10 cm) in order to hold the material in place. Then columns were packed with 27 g and 17 g CFH-12 with bed depths of 7 cm and 5 cm, respectively. The top layer of the column was filled up with quartz. The vanadium solution was pumped using a peristaltic pump from bottom to top with a flow rate of 2.6–2.7 mL/min (empty bed contact time: ~32 min).

After preliminary experiments with a synthetic vanadium solution, CFH-12, GEH 101 and GWTR-Peat were tested in the columns with real mining ditch water (initial vanadium concentration 6.85 mg/L; pH 7.02–7.83). The columns (same size as above) were packed similarly: first with quartz (height: 10 cm for CFH-12 and GEH 101, 3 cm for GWTR-Peat), then with 17 g of the sorbents (bed depths: 5 cm CFH-12, 4.5 cm GEH 101 and 23.5 cm GWTR-Peat) and finally with quartz on the top. Around 25 L of mining ditch water was fed to each column.

The column outflow solutions were collected for residual vanadium analysis using the phosphorus-tungsten-vanadium spectrophotometry method (UV-1800, Shimadzu) (Li, 2011). The breakthrough curve was obtained by plotting C_t/C_0 versus outflow volume, where C_t is the outflow vanadium concentration and C_0 is the inflow vanadium concentration. In order to predict the column sorption process, the experimental data were fitted with the Thomas (Eq. (7)) (Thomas, 1948) and Yoon-Nelson (Eq. (8)) (Yoon and Nelson, 1984) models:

$$\frac{C_t}{C_0} = \frac{1}{1 + \exp\left(K_{TH} \times q_0 \times \frac{m}{Q} - K_{TH} \times C_0 \times t\right)} \quad (7)$$

$$\frac{C_t}{C_0} = \frac{1}{1 + \exp[K_{YN}(\tau - t)]} \quad (8)$$

where C_0 is the inflow vanadium concentration (mg/L); C_t is the outflow vanadium concentration at a time of t (mg/L); K_{TH} is the Thomas rate constant (mL/(min × mg); q_0 is the maximum uptake capacity (mg/g); m is the mass of the sorbent in the column (g); Q is the flow rate of the solution (L/min); k_{YN} is the Yoon and Nelson rate constant (1/min); and τ is the time at which the outflow concentration is the half of the inflow concentration (min). All data were fitted and analysed in non-linear form. The Thomas model is based on the assumption that the process obeys the Langmuir kinetics of adsorption-desorption and the rate driving force follows second-order reversible reaction kinetics (Aksu and Gönen, 2004). In addition, the Thomas model does not consider axial dispersion. The Yoon-Nelson model is based on the assumption that the rate of decrease in the probability of adsorption for each adsorbate molecule is proportional to the probability of adsorbate breakthrough on the adsorbent (Aksu and Gönen, 2004).

3. Results and discussion

3.1. Health risk from exposure to vanadium in the ditch water

The vanadium concentration in the ditch water was 4.66–6.85 mg/L, a value well above some of the limits for vanadium in drinking waters (Crebelli and Leopardi, 2012; Wright and Belitz, 2010). Therefore, it was considered to be important to conduct a non-carcinogenic environmental risk assessment for people with potential exposure to this water. The calculated HQs from exposure to vanadium in the ditch water through ingestion and dermal contact routes were >1, which indicated that it was a risk for people with potential exposure to the water and in particular, from dermal contact (Table 2). Therefore, it is of utmost importance to treat the ditch water to decrease its vanadium content before it flows into recipient water bodies.

3.2. Characterization of the mining ditch water

The pH and conductivity of the mining ditch water were in the range of 7.02–7.83 and 201–235 μs/cm, respectively. Vanadium concentration varied between 4.66 and 6.85 mg/L. The variation was due to the two different sampling dates and slight changes were observed during water storage. Besides vanadium, mining ditch water also contained sulfate, chloride, iron, and some aluminium (Table 3, showing data for one sampled water batch). Thermodynamic calculations using MINEQL revealed that vanadium existed predominately in the 5+ valent form and in the form of $H_2VO_4^-$ (49.2–73.8%), $H_3V_2O_7^-$ (9.4–49.5%) and HVO_4^{2-} (0.8–14.6%) species under the prevailing pH 7.02–7.83 of the mining ditch water (Fig. 2). Several studies have shown that vanadium sorption is most efficient at lower pH values (3–4), and it is largely related to vanadium speciation and properties of the sorbent (Thamilarasi et al., 2018; Zhang et al., 2019; Zhang and Leiviskä, 2020). However, this study aimed at investigating vanadium removal from mining ditch water without the need for pH adjustment.

3.3. Characterization of fresh sorbents

FESEM micrographs of the fresh CFH-12 sorbent presented a coarse and porous surface, GEH 101 displayed a smoother surface with some smaller particles attached, and GWTR was porous and composed of

Table 2
HQ from exposure to vanadium in ditch water through ingestion and dermal contact. ADD is the average daily dose, RfD is the reference dose and DAD the dermal absorbed dose.

	ADD (mg/(kg × day))	RfD (ingestion) (mg/(kg × day))	HQ
Ingestion	0.074	0.007	10.53
	DAD (mg/(kg × day))	RfD (dermal) (mg/(kg × day))	HQ
Dermal	0.550	0.0014	392.56

Table 3
Characteristics of the mining ditch water before and after sorption (dosage 1 g/L; contact time 72 h).

Parameters (μg/L)	Mining ditch water	Water treated with sorbents			
		CFH-12	GEH 101	GWTR	GWTR-Peat
pH	7.58	7.47	7.78	7.49	7.21
Al	611	124	148	87.2	88.3
As	0.41	0.12	0.14	0.25	0.16
B	29.8	34.2	29.1	29.4	31.1
Ba	24.4	9.8	4.3	6.6	4.2
Be	0.076	<0.05	<0.05	<0.05	<0.05
Cd	0.016	<0.01	<0.01	<0.01	<0.01
Co	3.7	1.3	0.82	0.26	0.36
Cr	5.2	0.66	0.73	0.61	0.73
Cu	17.2	4.3	4.6	3.0	2.1
Fe	6070	1560	1810	2010	1390
Hg	<0.02	<0.02	<0.02	<0.02	<0.02
Mn	280	172	81.3	29.0	67.3
Mo	5.1	1.0	0.87	4.7	3.9
Ni	6.9	10	1.7	3.3	0.84
Pb	0.18	0.044	0.057	0.036	0.041
Sb	0.18	<0.05	<0.05	0.086	0.15
Se	0.23	<0.2	<0.2	<0.2	0.36
Sn	<0.05	<0.05	<0.05	<0.05	<0.05
Sr	57	60.5	41.1	42.0	16.8
Ti	<0.01	<0.01	<0.01	<0.01	<0.01
U	0.12	0.021	0.025	0.031	0.023
V	5380	658	631	409	880
Zn	6	2.6	0.82	1.1	0.88
Cl^-	12,000	10,900	22,200	10,700	11,000
F^-	300	<100	<100	<100	<100
SO_4^{2-}	56,000	103,000	56,400	58,700	60,500
NH_4^+	<10	<10	12	<10	40
NO_2^-	24	<10	<10	<10	<10
NO_3^-	1300	1700	1700	1500	860
PO_4^{3-}–P	20	9.6	9	76	35

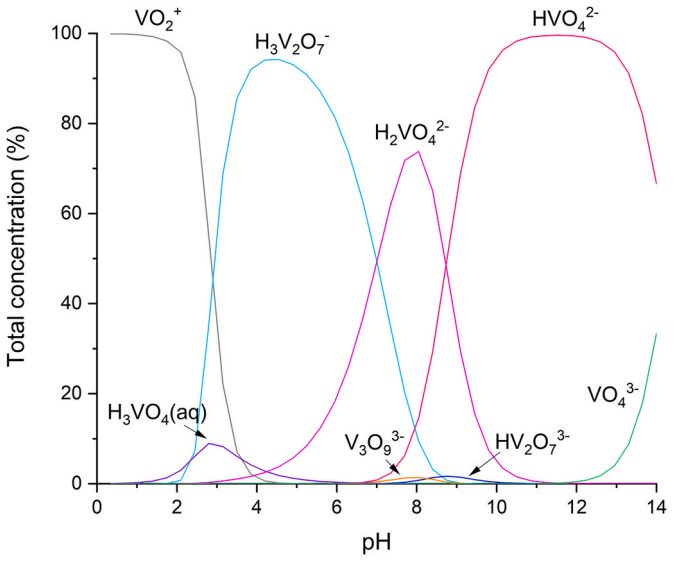

Fig. 2. Distribution of vanadium species as a function of pH in the mining ditch water (vanadium concentration: 0.106 mM). The pH of the mining ditch water was in the range of 7.02–7.83.

small spherical particles with large pores on the surface (Fig. 3).

The surface elemental composition of fresh sorbents showed that CFH-12, GEH 101 and GWTR contained Fe and O as major components, while GWTR-Peat contained C and O (Table 4). Small amounts of some other elements were also found in all the sorbents. The C 1s spectra of fresh sorbents (Fig. 6) showed three peaks for CFH-12 and GEH 101 that can be assigned to C–C/C–H (284.8 eV), C–O (286.1–286.2 eV) and inorganic carbonate/bicarbonate (289.2 ± 0.1 eV), respectively (Heuer and Stubbins, 1999; Sun et al., 2006). C–C/C–H and C–O components may have mostly originated from adventitious carbon and the inorganic carbonate/bicarbonate probably originated from the washing procedure. Fresh GWTR and GWTR-Peat presented three peaks: C–C/C–H (284.8 eV), C–O/C–N (286.4 ± 0.1 eV) and C–O–C/C═O (288.4–288.5 eV). The higher carbon content in the GWTR-Peat originated mainly from peat while the carbon in GWTR probably mostly arose from the natural organic matter originally present in the groundwater (Albrektiene et al., 2014). All of the fresh sorbents showed Fe–O (530.2 ± 0.2 eV) and –OH/C═O (531.4 ± 0.2 eV) in the O 1s spectra (Fig. S2).

3.4. Batch sorption tests

3.4.1. Effect of sorbent dosage

Vanadium was efficiently removed from the mining ditch water by all sorbents (Fig. 4), with the removal efficiency improving with increasing dosage. The removal efficiency was over 80% when the dosage was 4 g/L and increased to >90% with a dosage of 6 g/L for all sorbents. GWTR performed slightly better (84% removal) than the other three materials when using the lower dosage (1 g/L). This higher efficiency of GWTR was probably related to the fine powder form of GWTR and thus a greater number of easily accessible sites to bind vanadium. In addition, its higher average pore width (5.0 nm) compared to CFH-12 (3.3 nm) and GEH 101 (3.3 nm) and higher iron content (57.6%) compared to GWTR-Peat (14.6%; Table 1) might be further reasons for its superior sorption performance.

3.4.2. Effect of contact time

Vanadium removal efficiency from mining ditch water varied within the first hour for the different materials (CFH-12 48%; GEH 101 57%; GWTR 79%; and GWTR-Peat 61%), with the removal efficiency increasing with contact time to exceed 85% for all sorbents (72 h). The sorption efficiency for CFH-12, GWTR-Peat and GEH 101 was more influenced by the contact time. However, for GWTR, the removal efficiency was more stable and in the range of 79–92% with a contact time varying between 1 and 72 h. Faster sorption kinetics of GWTR compared to other studied sorbents was also observed in the experiments with synthetic vanadium solutions (Fig. S3). The higher efficiency of GWTR with a shorter contact time can be explained by its smaller particle size and consequent greater external surface area, as noted in section 3.3.1. It is also worth noting that all the selected sorbents efficiently removed vanadium from the mining ditch water with the presence of other predominant pollutants, i.e. Fe, Cl^-, and SO_4^{2-} (as shown in Table 3).

Reaching equilibrium was a slow process with all of the materials in both mining ditch water and synthetic vanadium solution, which can be attributed to the presence of amorphous iron material in the sorbents. Previous studies have demonstrated that CFH-12 is an amorphous ferric oxyhydroxide, GEH 101 contains amorphous ferrihydrite (Das et al., 2011), GWTR-Peat is mainly an amorphous material (Zhang et al., 2019), and the XRD analysis performed in this study showed the main components of GWTR to be amorphous (Fig. S4).

Sorption kinetics in the real mining ditch water were studied with different kinetic models (Fig. 5) and the parameters obtained are listed in Table 5. The experimental data were best described by the Elovich model, which has been extensively applied to chemisorption data (Roginsky and Zeldovich, 1934), and was also found to provide the best fit to the kinetic data for all the studied in vanadium sorption from synthetic solutions (Table S1 and Fig. S3).

For the mining ditch water, the plots of q_t *vs* $t^{0.5}$ from the intra-particle diffusion model showed relatively poor linearity for GEH 101, GWTR and GWTR-Peat (R^2 0.800–0.928), whereas CFH-12 presented better linearity (R^2 0.985) over the whole range. However, none of the plots pass through the origin (Fig. S5), which indicated that, for all the sorbents, the sorption process in real mining ditch water was not totally governed by intra-particle diffusion.

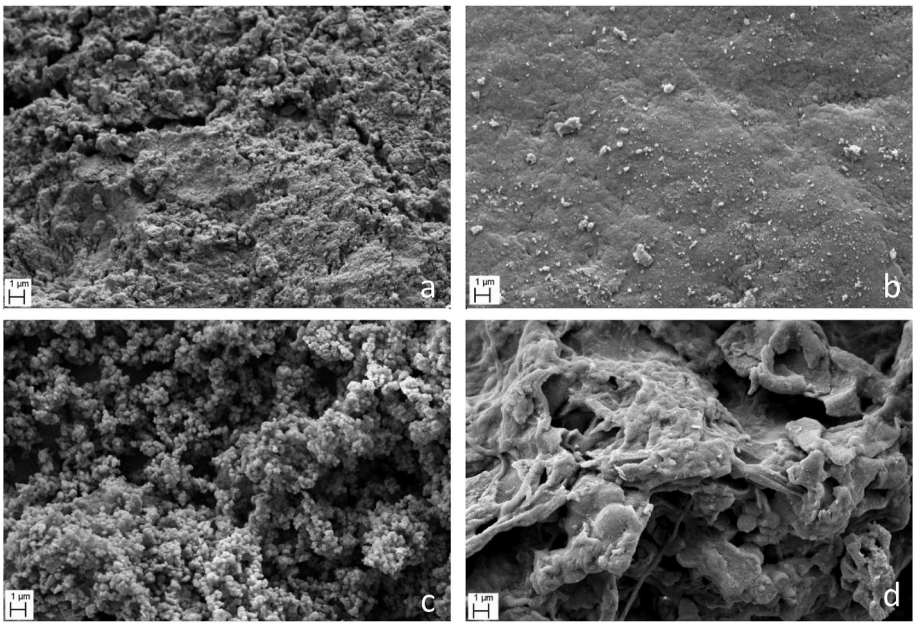

Fig. 3. FESEM images of fresh (a) CFH-12, (b) GEH 101, (c) GWTR, and (d) GWTR-Peat.

Table 4
Surface elemental composition (atomic %) of fresh and used sorbents.

	Fresh CFH-12	Used CFH-12	Fresh GEH 101	Used GEH 101	Fresh GWTR	Used GWTR	Fresh GWTR-Peat	Used GWTR-Peat
C 1s	2.5	14.7	7.7	13.3	8.6	8.2	43.1	46.4
O 1s	63.1	57.4	55.7	52.9	54.2	56.2	40.6	38.8
Fe 2p	28.5	22.5	32.0	29.4	22.7	22.1	8.4	7.3
Si 2p	2.8	2.8	1.6	2.0	6.0	6.4	3.4	2.8
Si 2s	–	–	–	–	6.1	5.0	2.3	2.1
S 2p	2.2	0.84	–	–	–	–	–	–
F 1s	0.89	0.69	1.3	1.2	0.62	0.44	–	–
N 1s	–	0.62	–	–	0.66	0.59	1.8	1.8
Cl 2p	–	–	1.7	0.9	–	–	–	–
P 2p	–	–	–	–	0.47	0.17	0.41	0.81
Mn 2p	–	–	–	–	0.44	0.83	–	–
Ca 2p	–	–	–	–	0.12	0.05	–	–
V 2p	–	0.50	–	0.26	–	–	–	0.05

For synthetic vanadium solution, the q_t *vs* $t^{0.5}$ plots of intra-particle diffusion model clearly presented two linear regions for all the sorbents, indicating that the sorption process was governed by different mechanisms (Fig. S6). The first linear region was related to the film diffusion process while the second region corresponded to intra-particle diffusion. Additionally, k_i values for all the sorbents in the first linear plots were higher than in the second linear plots (Table S1), which suggested that the reaction in the first stage (film diffusion) was faster compared to the second stage (intra-particle diffusion). Moreover, it should be noted that the ratio of $k_{i,1}/k_{i,2}$ was around 17 for GWTR, whereas the value was much lower (~2–3) for other three sorbents. This suggested the rapid chemical reaction with the abundant active sites of GWTR at the early stage.

Vanadium sorption kinetic data in synthetic solutions were further investigated by the Boyd model, which can reveal the rate-controlling step. The Boyd plots were linear and passed through the origin for all the sorbents at the sorption stage ($F \leq 0.85$) except for GWTR, for which the curve was linear but did not go through the origin (Fig. S7). This indicated that intra-particle diffusion was rate-limiting step for CFH-12, GEH 101 and GWTR-Peat at the sorption stage ($F \leq 0.85$), whereas film diffusion controlled the sorption rate for GWTR.

3.4.3. Water quality after sorption

All sorbents removed iron and aluminium to some extent from the mining ditch water along with elements existing with lower concentrations such as barium, cobalt, chromium, copper, manganese and zinc. However, it should be noted that a large amount of sulfate was leached from the gypsum impurity in CFH-12, as in agreement with previous studies (Leiviskä et al., 2017a, 2019). In addition, the chloride concentration increased in the treated water when using GEH 101. This was probably due to leaching of chlorine ions from GEH 101, as chlorine ions stabilize the akaganéite structure (Cai et al., 2001). With GWTR-based products, a very small amount of phosphate was leached that probably originated from the groundwater and was simultaneously precipitated with iron in the process. Nevertheless, none of the selected sorbents leached toxic or hazardous elements into the treated water, indicating that these four materials are safe to use. Additionally, leaching of impurities from CFH-12 and GEH 101 would eventually stop when using these products in multiple sorption-desorption cycles. It has been confirmed in a previous study that CFH-12 and GEH 101 can be regenerated and reused (Leiviskä et al., 2019).

3.4.4. Characterization of used sorbents

The FESEM images of used sorbents showed that there were no obvious differences between the fresh and used sorbents (Fig. S8). However, clear changes were observed in the XPS survey spectra of used sorbents compared to fresh ones. The sulfur content in CFH-12 and chlorine content in GEH 101 were lower in the used sorbents, whereas

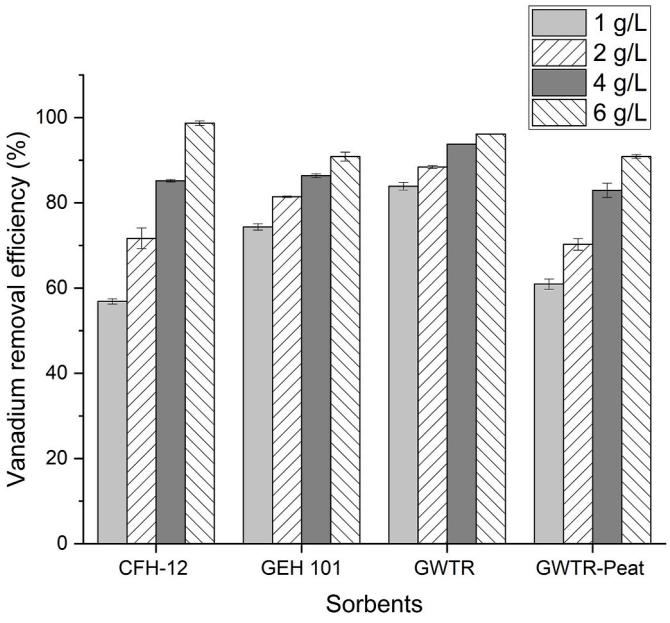

Fig. 4. Effect of dosage on vanadium removal efficiency (pH 7.02; contact time 24 h; initial vanadium concentration 4.66 mg/L; temperature 21 °C; error bars represent the range of two repeats).

the manganese content slightly increased in the used GWTR, which is in agreement with the water quality data after sorption (Table 3). However, the atomic % of Fe 2p decreased in all of the used materials (Table 4), which can be explained by the substantial increase in C 1s. Although some elements were found to be removed from the mining ditch water, many of them were not observed in the survey spectrum of the used sorbents. These included Al in all the used sorbents and Mn in the used CFH-12, GEH 101 and GWTR-Peat. Furthermore, the phosphorus content decreased only in the used GWTR, whereas it slightly increased in the used GWTR-Peat; this increase contradicts the observed leaching. However, a clear conclusion cannot be made due to the fact that the phosphate concentrations (Table 3) and the surface amounts (Table 4) were at very low levels and also because XPS is a surface-sensitive technique.

After the mining ditch water treatment, all of the used sorbents showed three peaks in C 1s spectra at 284.8 eV, 286.4 ± 0.1 eV, and 288.4–288.5 eV (Fig. 6), corresponding to C–C/C–H, C–O/C–N and C–O–C/C═O, respectively. In addition, carbonate/bicarbonate may still exist at around 290 eV in the used CFH-12 and GEH 101 and thus may be contained in the component on the higher BE side with C–O–C/C═O bonds. It was observed that the carbon content increased in the CFH-12, GEH 101 and GWTR-Peat samples, which was probably due to the sorption of organic compounds from the mining ditch water (Leiviskä et al., 2017b). This increase was mostly observed in the C 1s spectra as an increase in the middle and high BE component, especially with CFH-12 and GEH 101. Conversely, the carbon content in GWTR slightly decreased after treatment, which might be due to the washing and partial loss of the used GWTR and simultaneous washing of weakly bound organics from the material. The enriched carbon content in the used CFH-12, GEH 101 and GWTR-Peat may be related to the formation of strong bonds between the functional groups in the sorbents and organic compounds in the mining water. The result is in good agreement with previous studies whereby the sorption of organic compounds on iron sorbents may result in the formation of strong multiple bonds (Kaiser and Guggenberger, 2007; Leiviskä et al., 2017b).

An important mechanism for vanadium removal by iron materials is through the reaction between surface hydroxyl groups and vanadates (Leiviskä et al., 2019). After sorption, a new peak originating from the sorbed organic compounds was observed in O 1s spectra of CFH-12 and

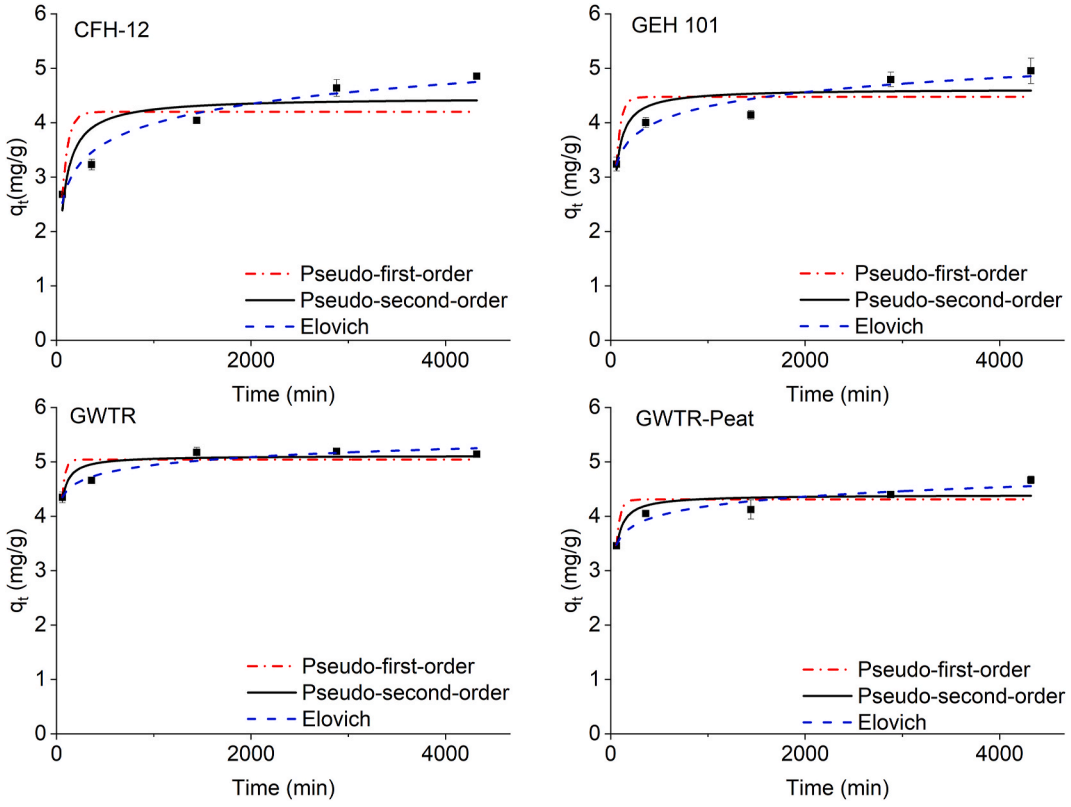

Fig. 5. PFO, PSO and Elovich kinetics by non-linear methods and experimental data for vanadium sorption from mining ditch water onto sorbents (dosage 1 g/L; solution pH 7.58; initial vanadium concentration 5.38–6.09 mg/L; temperature 21 °C; error bars represent the range of two repeats).

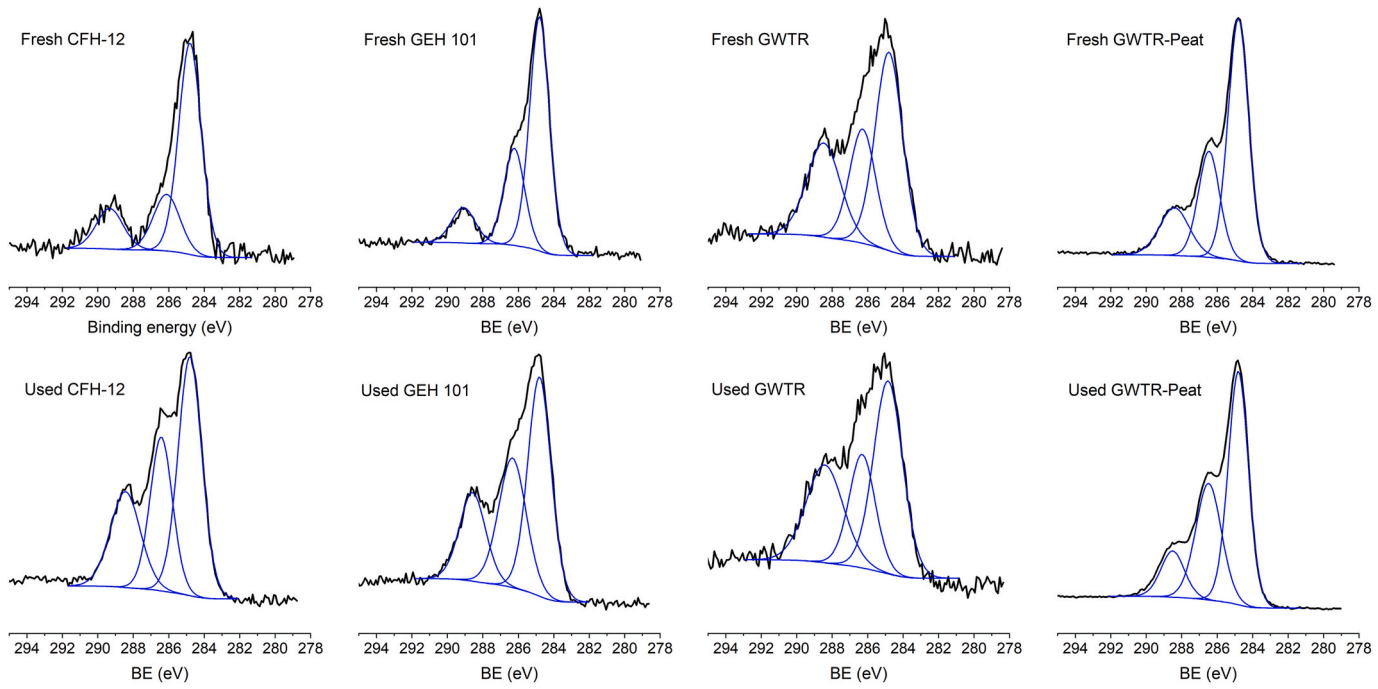

Fig. 6. C 1s spectra of fresh and used sorbents.

Table 5
Parameters of the PFO, PSO, Elovich and intra-particle diffusion (mining ditch water).

Models	Parameters	CFH-12	GEH 101	GWTR	GWTR-Peat
Pseudo-first-order	k_1 (1/min)	0.017	0.021	0.033	0.027
	q_e (mg/g)	4.2	4.5	5.0	4.3
	R^2	0.539	0.649	0.661	0.708
	χ^2	0.374	0.148	0.039	0.056
Pseudo-second-order	k_2 (g/mg × min)	0.004	0.008	0.017	0.013
	q_e (mg/g)	4.5	4.6	5.1	4.4
	R^2	0.745	0.778	0.805	0.808
	χ^2	0.227	0.094	0.000	0.036
Elovich	α (mg/(g × min))	1.096	30.156	3.2 E+6	4528
	β (g/mg)	1.9	2.6	4.7	4.0
	R^2	0.967	0.940	0.930	0.934
	χ^2	0.034	0.026	0.008	0.013
Intra-particle diffusion	k_i (mg/g × $min^{½}$)	0.038	0.028	0.014	0.018
	C	2.5	3.2	4.4	3.5
	R^2	0.985	0.928	0.800	0.901
	χ^2	0.013	0.036	0.006	0.022

GEH 101, whereas no obvious changes were observed in the O1s spectra of GWTR and GWTR-Peat (Fig. S2). Additionally, the middle component was increased, probably due to the increase of C═O bonds originating from sorbed organic compounds.

The used CFH-12 and GEH 101 showed V $2p_{3/2}$ and V $2p_{1/2}$ peaks at 516.9 eV and 524.2–524.3 eV, respectively (Fig. S9), indicating the existence of oxidized vanadium (V) on the surface of the used materials (Demeter et al., 2000); this agrees with a previous study using the same sorbents for vanadium sorption from synthetic vanadium solution (Leiviskä et al., 2019). However, GWTR-Peat showed relatively weak peaks at V $2p_{3/2}$ and V $2p_{1/2}$ compared to CFH-12 and GEH 101. Moreover, GWTR did not show a vanadium peak either in the survey spectrum or high resolution V 2p spectrum, which confirms that the washing procedure of the used GWTR sorbent before the analysis was not appropriate.

3.5. Column studies

In the column studies, GWTR was not tested due to its fine powder form. A preliminary test using a synthetic vanadium solution was conducted to estimate the performance of CFH-12. As shown in Fig. 7a, the bed depth had a significant impact on the performance, with the breakthrough time (normally taken as $C_t/C_0 = 0.1$) increasing from ~5900 to ~20,000 min when the dosage of CFH-12 was increased from 17 g to 27 g. Also, the shapes of the curves were slightly different with a less steep breakthrough curve and a higher bed depth. These results indicated that CFH-12 was capable of removing vanadium from a synthetic vanadium solution in a fixed bed column and that a higher bed depth provides a longer service time.

An early breakthrough was observed in all columns treated with the mining ditch water and a low concentration of vanadium was detected in the outflow within the first 2 h (Fig. 7b). The breakthrough time for CFH-12 (17 g) was observed much earlier when using mining ditch water (~100 min) compared to synthetic vanadium solution (~5900 min), as shown in Fig. 7c. This could be due to the complex composition of the mining ditch water as other pollutants might have competed with vanadium for the active sites. Pap et al. (2020) also reported a shorter breakthrough time with real wastewater compared to the synthetic

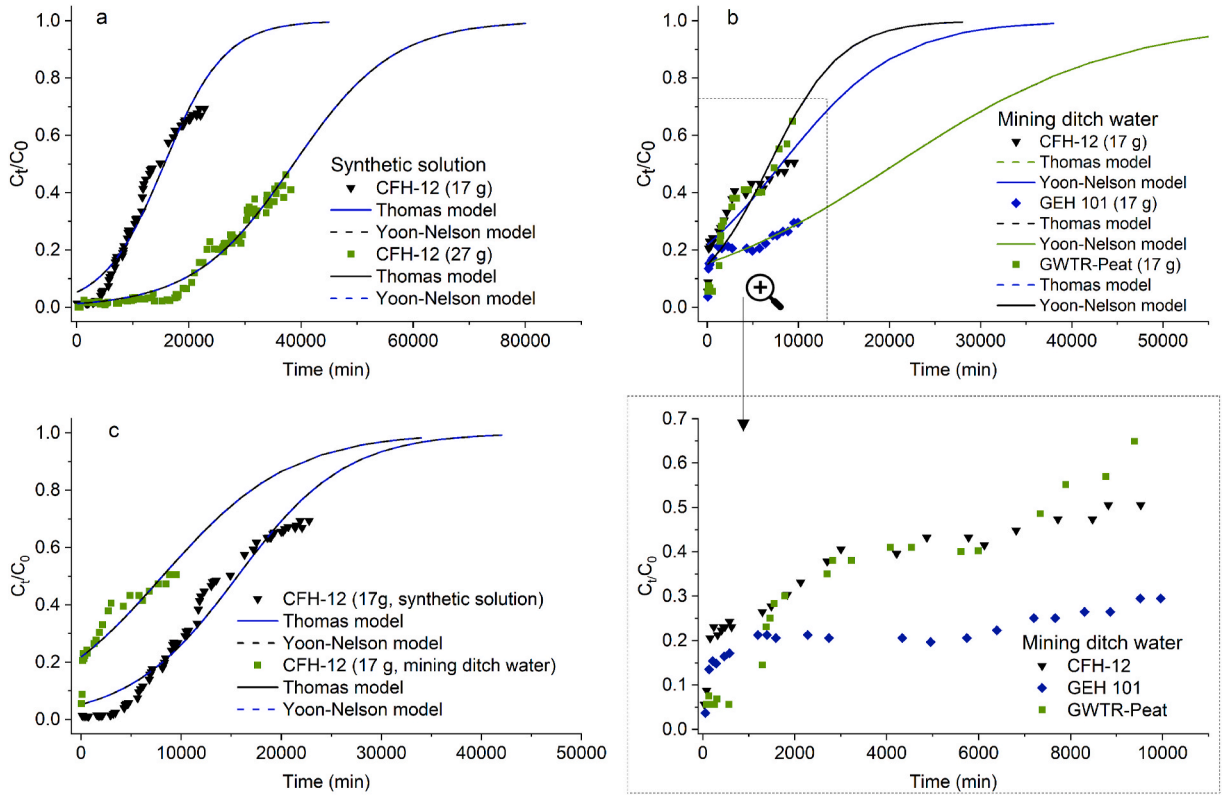

Fig. 7. Fixed-bed column experiments (flow rate 2.6–2.7 mL/min) for vanadium removal: (a) CFH-12 with synthetic solution (initial vanadium concentration C_0 5.18–6.75 mg/L; pH 6.0); (b) CFH-12, GEH-101, and GWTR-Peat with mining ditch water (C_0 6.85 mg/L; pH 7.02–7.83); and (c) a comparison of CFH-12 with synthetic solution (C_0 6.75 mg/L; pH 6.0) and mining ditch water (C_0 6.85 mg/L; pH 7.02–7.83).

Table 6
Parameters of Thomas and Yoon-Nelson models for CFH-12, GEH 101 and GWTR-Peat.

Models	Feeding solution	Synthetic solution		Mining ditch water		
	Sorbent	CFH-12	CFH-12	CFH-12	GEH 101	GWTR-Peat
	Sorbent mass	27 g	17 g	17 g	17 g	17 g
	Parameters					
Thomas	K_{TH} (mL/(min × mg))	0.022	0.027	0.023	0.012	0.037
	q (mg/g)	19.7	16.3	8.5	21.6	7.2
	R^2	0.963	0.955	0.804	0.682	0.832
	χ^2	0.601	1.008	0.294	0.137	0.783
Yoon-Nelson	K_{YN} (1/min)	1.1E-4	1.8E-4	1.6E-4	8.3E-5	2.6E-4
	τ (min)	38,642	15,610	8119	20,652	6836
	R^2	0.963	0.955	0.804	0.682	0.832
	χ^2	0.601	1.008	0.294	0.137	0.783

solution. In addition, the pH of mining ditch water (pH 7.02–7.83) was higher than that of synthetic water (pH 6) and therefore, likely affected the vanadium speciation and removal efficiency (see section 3.2). GEH 101 outperformed CFH-12 and GWTR-Peat in the column mode. For GEH 101, the 50% breakthrough ($C_t/C_0 = 0.5$) was not reached (>9959 min), with the amount of mining ditch effluent fed, whereas the 50% breakthrough was observed at around 8475 min and 7338 min for CFH-12 and GWTR-Peat, respectively. Moreover, the slope of the curve was less steep with GEH 101, indicating a longer mass transfer zone. Nevertheless, these results suggest that the studied sorbents can achieve good performance in the column mode as long as a longer contact time is provided. The column breakthrough time can be increased by decreasing the flow rate or increasing the bed depth (Bulgariu and Bulgariu, 2016; Han et al., 2009). The mining ditch water vanadium concentration was stable in this study due to batch sampling the water but in practice, the vanadium concentration can significantly vary under the field conditions. The initial pollutant ion concentration affects the breakthrough times (Bulgariu and Bulgariu, 2016) and should be taken into account in the design of the filter system.

The column data was analysed using the Thomas and Yoon-Nelson models (Table 6). The predicted maximum capacities (q, obtained from the Thomas model) were 19.7 mg/g for 27 g of CFH-12 and 16.3 mg/g for 17 g of CFH-12, which are somewhat lower than those obtained with synthetic vanadium solution (34 mg/g) in the batch mode and using a much longer contact time (72 h) (Leiviskä et al., 2019). The estimated τ (the time at which $C_t/C_0 = 0.5$) from the Yoon-Nelson model was 38,642 min for 27 g of CFH-12 and 15,610 min for 17 g of CFH-12, which was close to the experimental data. For the columns tested with mining ditch water, the parameters obtained from the Thomas and Yoon-Nelson models were quite reasonable, indicating a higher capacity and higher 50% breakthrough time for GEH 101. The τ was also close to the experimental data (in the case of CFH-12 and GWTR-Peat). The

estimated value does not differ significantly with the experimental value for all the columns (*t*-test, $p > 0.05$, two-tailed) at a confidence level of 95%, although a lower R^2 was obtained in the GEH 101 column. However, it should be noted that the estimated breakthrough curves from the Thomas and Yoon-Nelson models overlap, which has also been reported in previous studies (Li et al., 2016; Unuabonah et al., 2012).

4. Conclusions

The mining ditch water had a significant vanadium concentration and could pose a risk to human health based on the risk assessment. Commercial iron sorbents and low-cost sorbents derived from iron waste sludge proved to be efficient for vanadium removal from the mining ditch water. Vanadium removal efficiency improved with increasing dosage and contact time. Kinetic data suggested that both film diffusion and intra-particle diffusion were the rate-controlling processes. Batch studies revealed that all the selected sorbents were safe to be used for water purification since no toxic and hazardous elements were leached into the treated water under the studied conditions. GEH 101 provided a better performance in the column mode compared to CFH-12 and GWTR-Peat with higher efficiency being able to be obtained by optimization of bed depth and flow rate.

Declaration of competing interest

The authors declare that they have no known competing financial interests or personal relationships that could have appeared to influence the work reported in this paper.

Acknowledgements

This study was funded by the VanProd project “Innovation for enhanced production of vanadium from waste streams in the Nordic Region” and the Geovana project “Removal of vanadium from mining wastewaters and contaminated natural waters using geological materials” (2016-2019). The authors express their sincere thanks for the financial support from the European Union programme Interreg Nord 2014-2020, the Regional Council of Lapland and the K.H. Renlund Foundation.

Appendix A. Supplementary data

Supplementary data to this article can be found online at https://doi.org/10.1016/j.chemosphere.2021.131817.

Authors contributions

Ruichi Zhang: Conceptualization, Writing – original draft, Investigation, Visualization, Methodology. Jinmei Lu: Conceptualization, Writing – review & editing, Formal analysis, Visualization. Mark Dopson: Conceptualization, Writing – review & editing. Tiina Leiviskä: Conceptualization, Methodology, Writing – review & editing, Supervision, Funding acquisition.

References

Aksu, Z., Gönen, F., 2004. Biosorption of phenol by immobilized activated sludge in a continuous packed bed: prediction of breakthrough curves. Process Biochem. 39, 599–613. https://doi.org/10.1016/S0032-9592(03)00132-8.

Albrektiene, R., Rimeika, M., Voisniene, V., 2014. The characterisation of natural organic matter in ground water using rapid fractionation. WIT Trans. Ecol. Environ. 182, 111–120. https://doi.org/10.2495/WP140101.

Aryal, M., Ziagova, M., Liakopoulou-Kyriakides, M., 2010. Study on arsenic biosorption using Fe(III)-treated biomass of Staphylococcus xylosus. Chem. Eng. J. 162, 178–185. https://doi.org/10.1016/j.cej.2010.05.026.

Bello, A., Leiviskä, T., Zhang, R., Tanskanen, J., Maziarz, P., Matusik, J., Bhatnagar, A., 2019. Synthesis of zerovalent iron from water treatment residue as a conjugate with kaolin and its application for vanadium removal. J. Hazard Mater. 374, 372–381. https://doi.org/10.1016/j.jhazmat.2019.04.056.

Blanchard, G., Maunaye, M., Martin, G., 1984. Removal of heavy metals from waters by means of natural zeolites. Water Res. 18, 1501–1507.

Boyd, G.E., Adamson, A.W., Myers Jr., L.S., 1947. The exchange adsorption of ions from aqueous solutions by organic zeolites. II. Kinetics1. J. Am. Chem. Soc. 69, 2836–2848.

Bulgariu, D., Bulgariu, L., 2016. Potential use of alkaline treated algae waste biomass as sustainable biosorbent for clean recovery of cadmium(II) from aqueous media: batch and column studies. J. Clean. Prod. 112, 4525–4533. https://doi.org/10.1016/j.jclepro.2015.05.124.

Cai, J., Liu, J., Gao, Z., Navrotsky, A., Suib, S.L., 2001. Synthesis and anion exchange of tunnel structure akaganeite. Chem. Mater. 13, 4595–4602. https://doi.org/10.1021/cm010310w.

Castaldi, P., Silvetti, M., Garau, G., Demurtas, D., Deiana, S., 2015. Copper(II) and lead (II) removal from aqueous solution by water treatment residues. J. Hazard Mater. 283, 140–147. https://doi.org/10.1016/j.jhazmat.2014.09.019.

Çelebi, A., Şengörür, B., Kløve, B., 2014. Human health risk assessment of dissolved metals in groundwater and surface waters in the Melen watershed, Turkey. J. Environ. Sci. Heal. - Part A Toxic/Hazardous Subst. Environ. Eng. 49, 153–161. https://doi.org/10.1080/10934529.2013.838842.

Chen, A.S.C., Wang, L., Sorg, T.J., Lytle, D.A., 2020. Removing arsenic and co-occurring contaminants from drinking water by full-scale ion exchange and point-of-use/point-of-entry reverse osmosis systems. Water Res. 172, 115455. https://doi.org/10.1016/j.watres.2019.115455.

Chiang, Y.W., Ghyselbrecht, K., Santos, R.M., Martens, J.A., Swennen, R., Cappuyns, V., Meesschaert, B., 2012. Adsorption of multi-heavy metals onto water treatment residuals: sorption capacities and applications. Chem. Eng. J. 200– 202, 405–415. https://doi.org/10.1016/j.cej.2012.06.070.

Crebelli, R., Leopardi, P., 2012. Long-term risks of metal contaminants in drinking water: a critical appraisal of guideline values for arsenic and vanadium. Ann. Ist. Super Sanita 48, 354–361.

Dąbrowski, A., Hubicki, Z., Podkościelny, P., Robens, E., 2004. Selective removal of the heavy metal ions from waters and industrial wastewaters by ion-exchange method. Chemosphere 56, 91–106. https://doi.org/10.1016/j.chemosphere.2004.03.006.

Das, S., Hendry, M.J., Essilfie-Dughan, J., 2011. Transformation of two-line ferrihydrite to goethite and hematite as a function of pH and temperature. Environ. Sci. Technol. 45, 268–275. https://doi.org/10.1021/es101903y.

Demeter, M., Neumann, M., Reichelt, W., 2000. Mixed-valence vanadium oxides studied by XPS. Surf. Sci. 454, 41–44. https://doi.org/10.1016/S0039-6028(00)00111-4.

Dixit, S., Hering, J.G., 2003. Comparison of arsenic(V) and arsenic(III) sorption onto iron oxide minerals: implications for arsenic mobility. Environ. Sci. Technol. 37, 4182–4189. https://doi.org/10.1021/es030309t.

Edebali, S., 2019. Advanced Sorption Process Applications. BoD–Books on Demand.

Gao, S., Wang, C., Pei, Y., 2013. Comparison of different phosphate species adsorption by ferric and alum water treatment residuals. J. Environ. Sci. (China) 25, 986–992. https://doi.org/10.1016/S1001-0742(12)60113-2.

Giri, S.K., Das, N.N., Pradhan, G.C., 2011. Synthesis and characterization of magnetite nanoparticles using waste iron ore tailings for adsorptive removal of dyes from aqueous solution. Colloids Surfaces A Physicochem. Eng. Asp. 389, 43–49. https://doi.org/10.1016/j.colsurfa.2011.08.052.

Grace, M.A., Clifford, E., Healy, M.G., 2016. The potential for the use of waste products from a variety of sectors in water treatment processes. J. Clean. Prod. 137, 788–802. https://doi.org/10.1016/j.jclepro.2016.07.113.

Han, R., Wang, Yu, Zhao, X., Wang, Yuanfeng, Xie, F., Cheng, J., Tang, M., 2009. Adsorption of methylene blue by phoenix tree leaf powder in a fixed-bed column: experiments and prediction of breakthrough curves. Desalination 245, 284–297. https://doi.org/10.1016/j.desal.2008.07.013.

He, C., Zhang, B., Lu, J., Qiu, R., 2021. A newly discovered function of nitrate reductase in chemoautotrophic vanadate transformation by natural mackinawite in aquifer. Water Res. 189, 116664. https://doi.org/10.1016/j.watres.2020.116664.

Heuer, J.K., Stubbins, J.F., 1999. An XPS characterization of FeCO3 films from CO2 corrosion. Corrosion Sci. 41, 1231–1243.

Hu, J., Lo, I.M.C., Chen, G., 2004. Removal of Cr(VI) by magnetite nanoparticle. Water Sci. Technol. 50, 139–146.

Jacukowicz-Sobala, I., Ociński, D., Kociołek-Balawejder, E., 2015. Iron and aluminium oxides containing industrial wastes as adsorbents of heavy metals: application possibilities and limitations. Waste Manag. Res. 33, 612–629. https://doi.org/10.1177/0734242X15584841.

Janoš, P., Kopecká, A., Hejda, S., 2011. Utilization of waste humate product (iron humate) for the phosphorus removal from waters. Desalination 265, 88–92.

Kaiser, K., Guggenberger, G., 2007. Sorptive stabilization of organic matter by microporous goethite: sorption into small pores vs. surface complexation. Eur. J. Soil Sci. 58, 45–59.

Keränen, A., Leiviskä, T., Salakka, A., Tanskanen, J., 2015. Removal of nickel and vanadium from ammoniacal industrial wastewater by ion exchange and adsorption on activated carbon. Desalin. Water Treat. 53, 2645–2654.

Lagergren, S.K., 1898. About the theory of so-called adsorption of soluble substances. Sven. Vetenskapsakad. Handingarl 24, 1–39.

Lazaridis, N.K., Jekel, M., Zouboulis, A.I., 2003. Removal of Cr(VI), Mo(VI), and V(V) ions from single metal aqueous solutions by sorption or nanofiltration. Separ. Sci. Technol. 38, 2201–2219. https://doi.org/10.1081/SS-120021620.

Lee, T., Lim, H., Lee, Y., Park, J.W., 2003. Use of waste iron metal for removal of Cr(VI) from water. Chemosphere 53, 479–485. https://doi.org/10.1016/S0045-6535(03)00548-4.

Leiviskä, T., 2021. Vanadium (V) removal from water by sorption. In: Sorbents Materials for Controlling Environmental Pollution. Elsevier, pp. 543–571.

Leiviskä, T., Khalid, M.K., Sarpola, A., Tanskanen, J., 2017a. Removal of vanadium from industrial wastewater using iron sorbents in batch and continuous flow pilot systems. J. Environ. Manag. 190, 231–242. https://doi.org/10.1016/j.jenvman.2016.12.063.

Leiviskä, T., Leskelä, T., Tanskanen, J., 2019. Effect of alkali regeneration on pore characteristics and performance of ferric oxyhydroxide and akaganéite sorbents. J. Water Process Eng. 31, 100838. https://doi.org/10.1016/j.jwpe.2019.100838.

Leiviskä, T., Matusik, J., Muir, B., Tanskanen, J., 2017b. Vanadium removal by organo-zeolites and iron-based products from contaminated natural water. J. Clean. Prod. 167, 589–600. https://doi.org/10.1016/j.jclepro.2017.08.209.

Li, G.C., 2011. Determination of the vanadium in aqueous solution by phosphoric acid–sodium tungstate spectrophotometry method. J. Shanxi Coal Manag. Cadre Inst. 24, 141–143.

Li, Y., Li, L., Cao, L., Yang, C., 2016. Promoting dynamic adsorption of Pb2+ in a single pass flow using fibrous nano-TiO2/cellulose membranes. Chem. Eng. J. 283, 1145–1153. https://doi.org/10.1016/j.cej.2015.08.068.

Liu, H., Chen, T., Chang, J., Zou, X., Frost, R.L., 2013. The effect of hydroxyl groups and surface area of hematite derived from annealing goethite for phosphate removal. J. Colloid Interface Sci. 398, 88–94. https://doi.org/10.1016/j.jcis.2013.02.016.

López-Delgado, A., Pérez, C., López, F.A., 1998. Sorption of heavy metals on blast furnace sludge. Water Res. 32, 989–996. https://doi.org/10.1016/S0043-1354(97)00304-7.

Melita, L., Gumrah, F., 2010. Studies on transport of vanadium (V) and nickel (II) from wastewater using activated composite membranes. Waste Biomass. Valorizat. 1, 461–465. https://doi.org/10.1007/s12649-010-9031-9.

Pap, S., Kirk, C., Bremner, B., Turk Sekulic, M., Shearer, L., Gibb, S.W., Taggart, M.A., 2020. Low-cost chitosan-calcite adsorbent development for potential phosphate removal and recovery from wastewater effluent. Water Res. 173, 115573. https://doi.org/10.1016/j.watres.2020.115573.

Park, D., Lim, S.R., Lee, H.W., Park, J.M., 2008. Mechanism and kinetics of Cr(VI) reduction by waste slag generated from iron making industry. Hydrometallurgy 93, 72–75. https://doi.org/10.1016/j.hydromet.2008.03.003.

Roginsky, S., Zeldovich, Y.B., 1934. The catalytic oxidation of carbon monoxide on manganese dioxide. Acta Phys. Chem. USSR 1, 554.

Shi, J., Zhang, B., Cheng, Y., Peng, K., 2020. Microbial vanadate reduction coupled to co-metabolic phenanthrene biodegradation in groundwater. Water Res. 186, 116354. https://doi.org/10.1016/j.watres.2020.116354.

Sun, Y., Ding, X., Zheng, Z., Cheng, X., Hu, X., Peng, Y., 2006. Magnetic separation of polymer hybrid iron oxide nanoparticles triggered by temperature. Chem. Commun. 2765–2767. https://doi.org/10.1039/b604202c.

Teng, Y., Ni, S., Zhang, C., Wang, J., Lin, X., Huang, Y., 2006. Environmental geochemistry and ecological risk of vanadium pollution in Panzhihua mining and smelting area, Sichuan, China. Chin. J. Geochem. 25, 379–385.

Thamilarasi, M.J.V., Anilkumar, P., Theivarasu, C., Sureshkumar, M.V., 2018. Removal of vanadium from wastewater using surface-modified lignocellulosic material. Environ. Sci. Pollut. Res. 25, 26182–26191. https://doi.org/10.1007/s11356-018-2675-x.

Thomas, H.C., 1948. Chromatography: a problem in kinetics. Ann. N. Y. Acad. Sci. 49, 161–182.

Unuabonah, E.I., El-Khaiary, M.I., Olu-Owolabi, B.I., Adebowale, K.O., 2012. Predicting the dynamics and performance of a polymer-clay based composite in a fixed bed system for the removal of lead (II) ion. Chem. Eng. Res. Des. 90, 1105–1115. https://doi.org/10.1016/j.cherd.2011.11.009.

Wang, C., Yuan, N., Bai, L., Jiang, H.L., Pei, Y., Yan, Z., 2016a. Key factors related to drinking water treatment residue selection for adsorptive properties tuning via oxygen-limited heat treatment. Chem. Eng. J. 306, 897–907. https://doi.org/10.1016/j.cej.2016.08.037.

Wang, C.H., Gao, S.J., Wang, T.X., Tian, B.H., Pei, Y.S., 2011. Effectiveness of sequential thermal and acid activation on phosphorus removal by ferric and alum water treatment residuals. Chem. Eng. J. 172, 885–891. https://doi.org/10.1016/j.cej.2011.06.078.

Wang, T., Xu, X., Ren, Z., Gao, B., Wang, H., 2016b. Adsorption of phosphate on surface of magnetic reed: characteristics, kinetic, isotherm, desorption, competitive and mechanistic studies. RSC Adv. 6, 5089–5099.

Wang, Z., Zhang, B., He, C., Shi, J., Wu, M., Guo, J., 2021. Sulfur-based mixotrophic vanadium (V) bio-reduction towards lower organic requirement and sulfate accumulation. Water Res. 189, 116655. https://doi.org/10.1016/j.watres.2020.116655.

Watt, J.A.J., Burke, I.T., Edwards, R.A., Malcolm, H.M., Mayes, W.M., Olszewska, J.P., Pan, G., Graham, M.C., Heal, K.V., Rose, N.L., Turner, S.D., Spears, B.M., 2018. Vanadium: a re-emerging environmental hazard. Environ. Sci. Technol. 52, 11973–11974. https://doi.org/10.1021/acs.est.8b05560.

Weber, W.J., Morris, J.C., 1963. Kinetics of adsorption on carbon from solution. J. Sanit. Eng. Div. 89, 31–60.

Wright, M.T., Belitz, K., 2010. Factors controlling the regional distribution of vanadium in groundwater. Ground Water 48, 515–525. https://doi.org/10.1111/j.1745-6584.2009.00666.x.

Yang, J., Teng, Y., Wu, J., Chen, H., Wang, G., Song, L., Yue, W., Zuo, R., Zhai, Y., 2017. Current status and associated human health risk of vanadium in soil in China. Chemosphere 171, 635–643. https://doi.org/10.1016/j.chemosphere.2016.12.058.

Yoon, Y.H., Nelson, J.H., 1984. Application of gas adsorption kinetics I. A theoretical model for respirator cartridge service life. Am. Ind. Hyg. Assoc. J. 45, 509–516. https://doi.org/10.1080/15298668491400197.

Yusan, S., Doyurum, Akyil, S., 2008. Sorption of uranium(VI) from aqueous solutions by akaganeite. J. Hazard Mater. 160, 388–395. https://doi.org/10.1016/j.jhazmat.2008.03.009.

Zelmanov, G., Semiat, R., 2015. The influence of competitive inorganic ions on phosphate removal from water by adsorption on iron (Fe^{+3}) oxide/hydroxide nanoparticles-based agglomerates. J. Water Process Eng. 5, 143–152. https://doi.org/10.1016/j.jwpe.2014.06.008.

Zhang, B., Li, Y., Fei, Y., Cheng, Y., 2021. Novel pathway for vanadium(V) bio-detoxification by gram-positive lactococcus raffinolactis. Environ. Sci. Technol. 55, 2121–2131. https://doi.org/10.1021/acs.est.0c07442.

Zhang, R., Leiviskä, T., 2020. Surface modification of pine bark with quaternary ammonium groups and its use for vanadium removal. Chem. Eng. J. 385 https://doi.org/10.1016/j.cej.2019.123967.

Zhang, R., Leiviskä, T., Tanskanen, J., Gao, B., Yue, Q., 2019. Utilization of ferric groundwater treatment residuals for inorganic-organic hybrid biosorbent preparation and its use for vanadium removal. Chem. Eng. J. 361, 680–689. https://doi.org/10.1016/j.cej.2018.12.122.

Zhang, Y., Li, S., Wang, X., Li, X., 2015. Coagulation performance and mechanism of polyaluminum ferric chloride (PAFC) coagulant synthesized using blast furnace dust. Separ. Purif. Technol. 154, 345–350. https://doi.org/10.1016/j.seppur.2015.09.075.